Journal of Materials Chemistry A

Accepted Manuscript

ROYAL SOCIETY OF CHEMISTRY

www.rsc.org/materialsA

Facile fabrication of porous carbon nanofibers by electrospun PAN/dimethylsulfone for capacitive deionization

Haojie Pan [a], Jianmao Yang [b], Shiping Wang [a], Zhubiao Xiong [a], Wenshu Cai [a], Jianyun Liu [a] *

[a] *College of Environmental Science and Engineering, State Environmental Protection Engineering Center for Pollution Treatment and Control in Textile Industry, Donghua University, Shanghai 201620, China*

[b] *Research Center for Analysis & Measurement, Donghua University, Shanghai 201620, PR China*

* Corresponding author: Tel: 86-21-67792381; Fax: 86-21-67792522. *E-mail:* jianyun.liu@dhu.edu.cn (J. Liu);

Abstract: This paper reports a facile method to fabricate porous carbon nanofibers (PCNFs) via electrospinning polyacrylonitrile/dimethylsulfone (PAN/DMSO2) pristine fiber followed by preoxidation and carbonization. The nanopores were produced due to the removal of DMSO2 during the preoxidation process of the nanofibers, without additional chemical or physical activation process involved. The specific surface and pore density were tunable by varying the PAN/DMSO2 ratio. The variation in structure and composition of the nanofibers after heat treatment was characterized by scanning electron microscopy, fourier transform infrared spectroscopy and energy dispersive X-ray spectroscopy. As a free-standing electrode material in electrochemical capacitor, the PCNFs showed an enhanced electrical double layer capacitance characteristic, confirmed by cyclic voltammetry. The PCNFs were used successfully for capacitive deionization (CDI) with the enhanced desalination amount of 8.1 mg/g, 4.5 times higher than that of

the pure PAN-based CNF. The good stability demonstrated this porous carbon nanofiber could be deployed for CDI application.

Keywords: Capacitive deionization, electrospinning, porous carbon nanofiber, dimethyl sulfone

1. Introduction

Capacitive deionization (CDI), also called capacitive desalination, has attracted much attention as one of the most promising techniques to produce the fresh water from saline water such as brackish water or wastewater[1-4]. The physical principle of CDI is based on the formation of the electrical double layer at an electrode–electrolyte interface under an applied voltage, by which the ions in the feed water are adsorbed on the electrode surface so that the water is purified[1]. During the discharge process, the ions are desorbed and the electrodes are regenerated. Compared to reverse osmosis[5, 6] and electrodialysis[7], this technique has many unique characteristics such as low energy consumption, cost effectiveness, low fouling/scaling potential and environment-friendly features[8-10]. The key factors that control the capacitance and desalination performance of the devices are the specific surface area, ionic transportation in the conductive porous electrode materials[11] and the coulomb efficiency (also called charge efficiency)[12]. Porous carbon-based electrode materials have been subjected to intensive studies for CDI applications due to their excellent chemical stability, high conductivity, high specific surface area and low cost. Different types of carbon materials, such as activated carbon[13, 14], carbon aerogel[15-17], carbon nanotubes[18, 19], graphene[20-22] and carbon nanofibers[23, 24] have been employed as electrode materials in order to enhance the desalination

performance. Among them, carbon nanofibers have a lot of advantages, such as superior mechanical characteristic and easy to prepare so that they can be directly fabricated into free-standing electrode materials without further processing. And the carbon nanofiber electrode can maintain good electrical conductivity since no polymeric binding agents are added which are known to reduce the conductivity of the electrodes. Electrospinning is a simple and versatile technique for generating carbon nanofibers (CNF) with the components variable in the precursor solution[25]. Polyacrylonitrile (PAN) is generally used as an electrospinning material to produce pristine nanofibers due to the good spinnability and considerable carbon yield[26-28]. However sole PAN-based nanofibers exhibit low surface area due to the shrinkage of fiber during the high temperature treatment process[24]. The additional activation processes such as physical [23, 29-33] and chemical post-treatment[28, 34] are often necessary to enhance the specific surface area of the nanofibers. Another way to fabricate the PAN-based porous CNF is to use polymethyl methacrylate (PMMA), polystyrene (PS), polyvinyl alcohol (PVA) or Nafion as sacrificial components to blend with PAN[35-37]. During the carbonization process of the electrospun fiber, these components readily decompose and disappear to create pores due to phase separation so that the porous carbon nanofibers could be obtained. The latter strategy is preferable due to the fine-tunability of pore structure by changing the amount of the sacrificial components and the simplicity of the process without additional treatment. However, serious phase separation usually results in nonuniform macro-porous structure, which limits the charge storage ability, being undesirable for the capacitor-related electrode materials[38]. Meanwhile, a large amount of reagents have to be

burned out, resulting in high cost and environmental pollution. Hence, selecting the appropriate reagents as additives to fabricate the meso/micro carbon materials is still of interest to researchers.

Dimethyl sulfone (DMSO2), as a high temperature solvent, exists in a crystal state at room temperature. PAN can be dissolved in the DMSO2 solvent with good compatibility at high temperature. The PAN foam and the final macroporous carbon monoliths have been fabricated based on the phase separation of DMSO2 and PAN at room temperature [39, 40]. But for capacitor application, the suitable micro/meso pore distribution in carbon materials is necessary in order to enhance the ion storage capacity and facilitate the ionic transportation[38].

In this paper, DMSO2 was used as the pore-forming agent, for the first time, to fabricate the PAN/DMSO2 nanofiber via electrospinning PAN/DMSO2 mixture in DMF solution. Based on the evaporation property of DMSO2 under the moderate temperature, the uniform meso/micro pores can be formed in the nanofibers during preoxidation stage of PAN, without the need of an additional treatment. Furthermore, the pore density is tunable by changing the PAN/DMSO2 ratio in solution. In addition, the process is cost effective since DMSO2 can be easily recovered and recycled [41]. After carbonization, the obtained well-defined porous carbon nanofiber (PCNF) web can be used directly as a free-standing electrode material for CDI. The electrochemical behavior and CDI desalination properties of the PCNFs were studied with excellent ionic transportation performance obtained due to the suitable pore distribution. The successful application of sublimating compounds in electrospun nanofibers may provide a new scalable

environmental-friendly route for fabrication of porous carbon electrode material with low cost.

2. Materials and methods

2.1 Preparation of porous carbon nanofiber (PCNF)

0.937 g polyacrylonitrile (PAN, MW=150000, Aldrich, 99.8%) was dissolved in 10 mL N,N-dimethyl formamide (DMF, MW=73, Sinopharm Chemical Reagents, 99.5%) to prepare 9 wt% PAN solution by gently stirring at 60 °C for 12 h. Then 0.625 g dimethylsulfone powder (DMSO2, MW=94, Aldrich, 98%) was added into the upper PAN solution and stirred again at room temperature to form the homogeneous precursor solution with the final mass ratio (PAN/DMSO2) of 3:2. By adjusting the addition amount of DMSO2, the precursor solutions with different mass ratios (PAN/DMSO2=3:2, 1:1, 2:3) were used for electrospinning. The PAN solution without DMSO2 addition (PAN/DMSO2=1:0) was used to prepare the control sample.

For electrospinning, the precursor solution was transferred into a 10 mL syringe with 25 gauge stainless steel needle through which the solution was pushed by a syringe pump (Baoding Longer Precision Pump Co., Ltd, China). The anode of the high-voltage power supply (DW-P303-1ACF0, Dongwen High Voltage, Tianjin, China) was connected to the syringe needle tip, and the cathode was connected to an Al foil, which is electrically connected to the ground. The electrospun fibers were collected on the Al foil. The electrospinning parameters, including voltage, flow rate of solution and the distance between nozzle to collector were carefully adjusted in order to get the uniform and continuous fibers. The optimal electrospinning conditions are as follows: the applied

voltage of 12 kV, flow rate of 1 mL/h and a receiving distance of 15 cm. The nanofiber (NF) was obtained at room temperature with the humidity below 30%. The as-electrospun pristine nanofibers prepared from the PAN/DMSO2 solution with different mass ratio (1:0, 3:2, 1:1, 2:3) were denoted as pristine NFs (1:0, 3:2, 1:1, 2:3), respectively.

The resultant pristine nanofiber webs corresponding to different PAN/DMSO2 mass ratio were placed into the furnace for preoxidation. DMSO2 in the nanofibers was sublimated by heating to 80 °C at a rate of 4 °C/min and holding at this temperature for 1 h. Then it was raised till 260 °C for 1 h to get the pre-oxidized NFs. Finally, the preoxidized NFs (1:0, 3:2, 1:1, 2:3) were heated to 800 °C at a rate of 5°C/min under the continuously flowing nitrogen atmosphere. After being held at this temperature for 1.5 h, the sample was cooled down under the nitrogen. Then the porous carbon nanofiber (PCNF) was obtained. The carbonized NFs derived from the different pristine NFs (1:0, 3:2, 1:1, 2:3) were denoted as PCNFs (1:0, 3:2, 1:1, 2:3), respectively. In order to demonstrate the feasibility of DMSO2 recovery, the proof-of-concept experiment was carried out by heating the PAN/DMSO2 pristine fiber in a self-made container (see Supporting Information (SI)).

2.2 Characterization methods

The microstructure and the surface morphology of the nanofibers were observed using a field emission scanning electron microscope (FE-SEM, S-4700, Hitachi Co., Ltd, Japan) operated with an acceleration voltage of 5 kV and current of 10 μA after coating the samples with platinum using a vacuum sputter coater. In order to determine the elemental composition in the NFs, energy dispersive X-ray (EDX) spectroscopy being attached to

SEM was scanned under the condition of an acceleration voltage of 10 kV and current of 20 μA.

Fourier transform infrared spectroscopy (FTIR, ThermoFisher Nicolet iN10 MX spectrometer, USA) was employed to investigate the chemical structure of components in the fiber by analyzing the vibration band from 4000 to 400 cm^{-1} with the spectral resolution of 4 cm^{-1}. The samples were prepared by mixing the nanofibers with KBr with the mass ratio of about 1:100. After being grounded, the obtained fine particles were pressed into sheet under the pressure of 8 MPa for FTIR measurement.

The pyrolysis of the pristine NF was determined by thermogravimetric analyzer (TGA, Mettler Toledo TGA 1). About 5 mg of sample was taken in a standard aluminum cup and heated from 30 °C to 300 °C at a heating rate of 1 °C/min in air.

The specific surface area was measured by the nitrogen adsorption with an accelerated surface area and porosity analyzer (MicromeriticsASAP2020, USA). The porosity parameters of the PCNFs were determined from nitrogen (77 K) adsorption/desorption isotherms. The specific surface area was calculated using the conventional BET method, and the pore size distribution was analyzed based on QSDFT (quenched solid density functional theory) methods since this method is more appropriate for the analysis of micro-mesoporous materials, as demonstrated in the literatures[42, 43].

2.3. Capacitor assembly and desalination test

The above prepared PCNF web was cut into a 60 mm × 40 mm size (~85 mg), and the two electrodes in parallel were assembled into the CDI cell. The titanium mesh was used as current collector which was connected with the power supply. The silicon gasket was

used to seal the cell. The Nylon mesh with the thickness of 0.84 mm was used as a spacer to provide the cell volume between two electrodes for water flowing. The CDI cell structure was shown in Fig. S3. The assembly should be careful in order to keep the same compression by using the same parts and same screwing. The desalination experiment of the capacitor was performed in a 0.5 g/L NaCl aqueous solution (50 mL) at room temperature by constant current (current density 50 mA/g) charge and short-circuit discharge mode controlled with a battery test system (LANHE, CT2001A, Wuhan, China). The test solution was circulated by a peristaltic pump with the flow rate of 10 mL/min.

Cyclic voltammetry (CV) were carried out using a Princeton 2273 electrochemical system with two-electrode configuration (same as the capacitor cell) in 58.5 g/L and 0.5 g/L NaCl solution, respectively. The specific capacitance (C_s) was calculated from CV curve based on the formula[44]:

$$C_S = \frac{1}{2m\Delta U v}\int_{U_0}^{U_0+\Delta U} I(U)dU \quad (1)$$

Where C_s: the specific capacitance (F/g), I: current (A), v: scan rate (V/s), m: the mass of the electrode (g), ΔU: the potential range got from CV (V).

NaCl concentration was obtained from ion conductivity according to a calibration curve of ion conductivity (μS cm^{-1}) and NaCl concentration (mg/L) made prior to the experiment. The relationship that ion conductivity is about two times the concentration of NaCl at room temperature was obtained. The ion conductivity was continuously monitored by using an ion conductivity meter. The final desalinization amount was calculated based on the following equation[45]:

$$Q = \frac{(c_0 - c_e)V}{2m} \quad (2)$$

Where Q: the desalinization amount (mg/g), c_0 and c_e are the initial and final NaCl concentration in the solution (mg/L), respectively; V: the volume of the solution used in the measurements (L), m: the mass of the electrode (g).

3. Results and Discussion

3.1. Surface Morphology and Structure Analysis

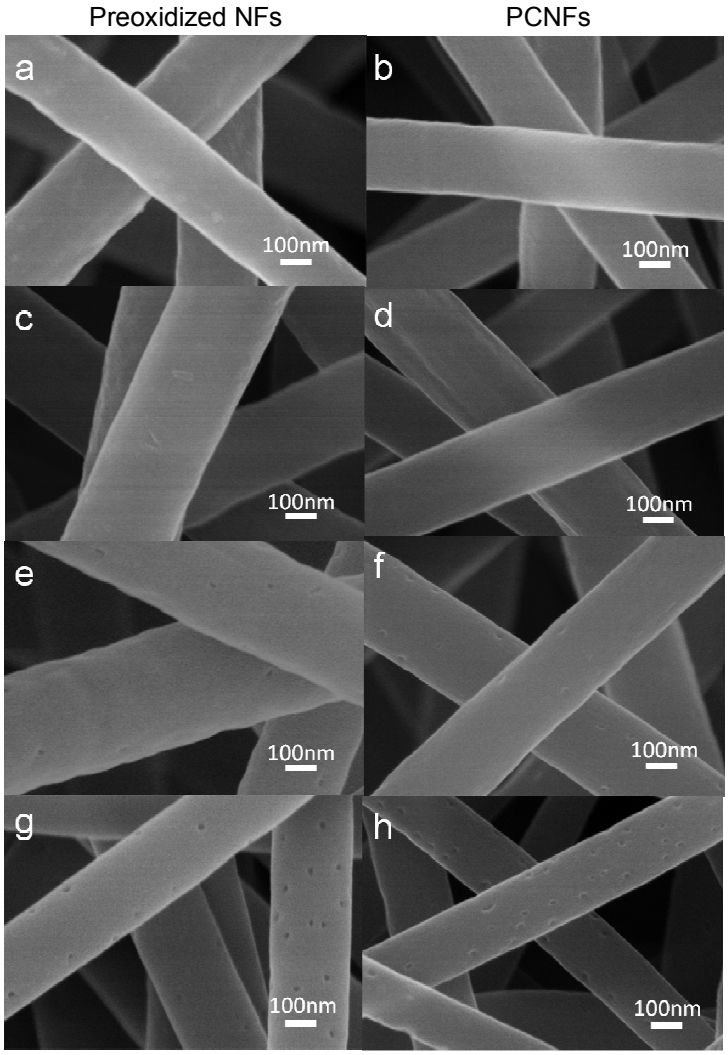

Fig. 1. SEM micrographs of the preoxidized NFs (a, c, e and g) and the corresponding PCNFs (b, d, f

and h) produced with the PAN/DMSO2 ratio of 1:0 (a,b), 3:2(c,d), 1:1(e,f) and 2:3 (g,h).

In the electrospinning process, PAN and DMSO2 were solidified into NFs accompanied with the evaporation of DMF solvent. The obtained PAN/DMSO2 pristine NFs (2:3) in comparison with pure PAN-based pristine NFs (1:0) presented a rough surface due to crystallization and phase separation of PAN and DMSO2 at room temperature (Fig. S4). While the preoxidized and carbonized NFs surface became smooth because of melting and evaporation of DMSO2. Fig. 1 exhibited the SEM images of the preoxidized NFs with different blend ratios of PAN/DMSO2 and the corresponding PCNFs. As shown in Fig.1, the control one (1:0) showed a uniform and smooth surface with the diameter distribution in the range of 250-300 nm (pattern a and b). With the addition of DMSO2, there was no obvious change on nanofiber diameter, but the nanopores were clearly observed along the nanofiber surface (pattern c, e and g) due to the escape of DMSO2. After carbonization, the obtained PCNFs (3:2, 1:1, 2:3) still kept the porous structure, even though the nanofibers became a bit thin due to shrinkage of the fibers (pattern d, f and h). Interestingly, the pore size increased with the increase in DMSO2 amount. We are thus able to control the pore size distribution of nanofibers by adjusting the DMSO2 amount.

DMSO2 is a thermally evaporable compound [39], so that DMSO2 in the PAN/DMSO2 nanofibers can be easily evaporated at a mild temperature and recrystallized for reuse. The recrystallization process was conducted with the simple self-made setup (Fig. S1 in SI) and the crystalized product was confirmed to be DMSO2 molecules by FTIR characterization (Fig. S2 in SI).

In order to investigate the release of DMSO2 during preoxidation process, FTIR spectra of the nanofibers with different PAN/DMSO2 ratio were scanned as shown in Fig. 2A. The spectrum of the pristine NF (1:0) exhibited the peaks at 2934, 2240 and 1470 cm^{-1} due to C-H stretching vibration of methylene, stretching vibration of nitrile groups (-CN-) and bending vibration of methylene in PAN, respectively. The band at 1640 cm^{-1} was ascribed to stretching vibration of C=O group possibly from the residual DMF solvent in the fiber or from the hydrolyzed PAN [46]. As to the DMSO2-containing pristine NFs (3:2, 1:1, 2:3), the noticeable peaks at about 1141 cm^{-1} and 1295 cm^{-1} corresponded to the typical O=S=O symmetric and asymmetric stretching vibration of DMSO2 [47], respectively. It indicates that DMSO2 was deposited in the electrospun nanofibers successfully. The absorption strength gradually increased with increasing the DMSO2 amount. The S=O bands disappeared (curve e) for the preoxidized NF(2:3) owing to the evaporation of DMSO2 during thermal treatment. The peak at 2247 cm^{-1} corresponding to C≡N stretching vibration became pretty weak, and a new band was formed at round 1601 cm^{-1} corresponding to N-H, C=C vibration. Meanwhile, the intensity of the C-H band of methylene at 2934 cm^{-1} decreased. All these demonstrate the successful cyclization of PAN during the preoxidation process, which contributes to the formation of the flexible fiber. EDX analysis in Fig. 2B showed an obvious S signal at 2.3 KeV (solid line in Fig.2B) in the pristine NF(2:3), but the element S signal disappeared after preoxidation of the nanofibers. It further confirms that DMSO2 was fixed in the fiber during the electrospinning process, while escaped from the nanofiber during the preoxidation stage. As a result, the pores were formed in the nanofiber, as

demonstrated in the above SEM images.

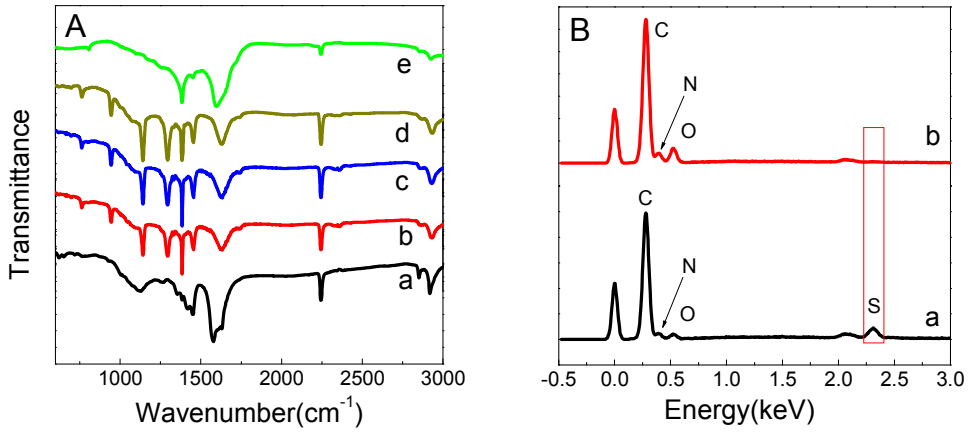

Fig.2. (A) FTIR spectra of pristine NFs (1:0(a), 3:2(b), 1:1(c), 2:3(d)) and preoxidized NF (2:3(e)). (B) EDX analysis of pristine NF(2:3(a)) and preoxidized NF(2:3(b)).

The thermo gravimetric analysis measurement was conducted in order to reveal the evaporation of DMSO2. Fig.3 gave the thermo gravimetric curves for different pristine NFs sample. For the pristine NF(1:0) sample, there was a slight weight loss at ~100°C owing to the release of DMF from the fiber, whereas for DMSO2-containing pristine NF, a sharp loss in weight was found at the temperature over 80 °C due to sublimation of DMSO2, indicating much DMSO2 on the nanofiber surface was removed at this moderate heating stage. With the increase of DMSO2 ratio in the fiber, high weight less was obtained. As demonstrated in SI (Table S1), DMSO2 could be recovered at this stage. Therefore, the higher weight loss indicates the higher recovery amount of DMSO2. Following a plateau at 130~240°C, there was second stage weight loss. For pristine NF(1:0), the second stage weight loss started at 260 °C owing to the cyclization of PAN, while the weight loss of DMSO2-containing pristine NFs (3:2, 1:1, 2:3) began at about

240°C. It is possible that the rest of DMSO2 trapped into the interior of nanofibers escaped when reaching the boiling point (238℃) of DMSO2. Finally, the pores were left. These results coincide with the SEM images, in which the higher the DMSO2 content was, the more the pores became. We conclude that the porous structure in the nanofibers is facilely constructed during the preoxidation process owing to the release of DMSO2.

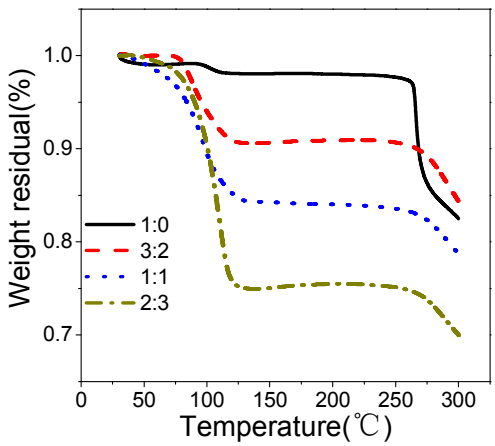

Fig.3. (A) Thermo-gravimetric curves of pristine NF (1:0, 3:2, 1:1, 2:3).

The pore characteristics of the PCNFs were measured by nitrogen adsorption-desorption test. The nitrogen sorption isotherms and pore size distributions of the carbons derived from PCNF (1:0, 3:2, 1:1, 2:3) were shown in Fig. 4A and Fig. 4B, respectively. The adsorbed volume of the pure PAN-based PCNF(1:0) was pretty low, indicating its nonporous characteristics. With the addition of DMSO2, the resultant PCNFs (3:2, 1:1, 2:3) exhibited a drastic uptake of nitrogen at low relative pressure, which is indicative of the presence of abundant micropores. A little uptilting at the higher relative pressure (>0.9 P/P_0) of the isotherm is probably due to the adsorption from mesopores on the outer surface of the fiber or the non-uniformity of the pore distribution. It confirms that the evaporation of DMSO2 during thermal treatment plays a key role to

produce the pores. The porosity parameters for all samples were summarized in Table 1 with BET surface area and pore structure information obtained from QSDFT simulation mode. It is worth noting that the BET specific surface area and total pore volume decreased with an increase in DMSO2 content in the fiber, whereas the fraction and average size of mesopores increased correspondingly (Table 1 and Fig.4B), which is in agreement with SEM image of fibers (*vide supra*). Presumably, in the PAN/DMSO2 fiber, DMSO2 crystals were distributed like "islands" in the PAN phase. The size of the "islands" can be fine-tuned by changing the DMSO2 content. The low DMSO2 content results in the formation of micropores structure during DMSO2 evaporation, whereas higher DMSO2 content results in more mesopores due to the tendency to accumulation and crystallization of DMSO2 molecules. The micro pores provide more sites for ion adsorption, but the meso pores facilitate the ionic transportation across the channel [48], which is more beneficial to CDI process (*vide infra*).

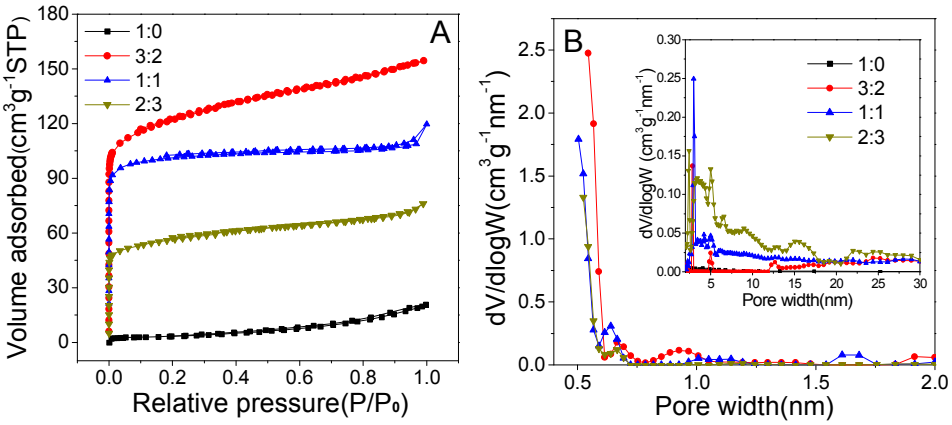

Fig.4. (A) N_2 adsorption-desorption isotherms and (B) Micro-pore size distributions of the PCNFs (1:0, 3:2, 1:1, 2:3) calculated from QSDFT method. Insert in pattern (B) is the meso pore size distribution of PCNF.

Table 1 Pore characteristics of the porous carbon nanofibers

Samples	S^a (m^2g^{-1})	V_T [b] (cm^3g^{-1})	V_{meso} (cm^3g^{-1})	V_{micro} (cm^3g^{-1})	Average Pore size (nm)	V_{meso}/V_T
PCNF(1:0)	12.2	0.032	0.0032	0	-	-
PCNF(3:2)	462	0.221	0.018	0.203	1.84	8.3%
PCNF(1:1)	402	0.157	0.041	0.116	2.07	25.7%
PCNF(2:3)	212	0.118	0.05	0.068	2.22	42.4%

[a] BET surface area, [b] total pore volume

3.2. Electrochemical characterization

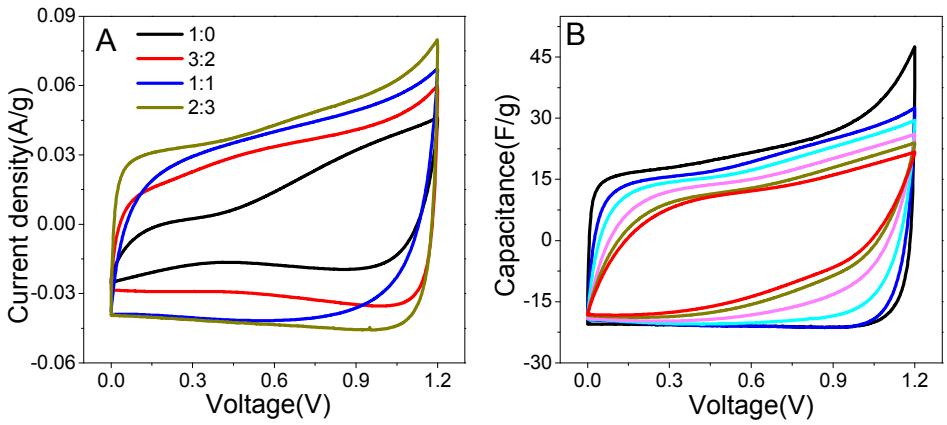

Fig.5. (A) CVs of the PCNFs electrodes, scan rate: 2 mV/s; (B) Normalized CV curves of PCNF (2:3) electrode in 58.5 g/L NaCl at different scan rates (from outside to inside: 1, 5, 10, 20, 30 and 40 mV/s).

The capacitance property of electrodes was evaluated by CV using a two-electrode system. Fig.5A presents the CV curves of the PCNF electrodes in 58.5 g/L NaCl solution at a scan rate of 2 mV/s. The near rectangular shape of the CV curve for PCNF electrode represents the charging – discharging process of a typical electric double layer capacitor. With increasing the DMSO2 content, more ideal rectangular curves were obtained. It suggests that the rich pores in the PCNF facilitate the ion diffusion and transportation along the pores, being consistent with the surface porosity analysis above. While, PCNF(1:0) showed a pretty low capacitance current. The specific capacitances C_s were

calculated from CV curve based on the formula (1) and the results were collected in Table 2. Clearly, the C_s value of the PCNF(1:0) electrode was only 16.1 F/g. However, the PCNF electrodes derived from DMSO2-containing NFs had much higher C_s value than PCNF(1:0) electrode. The higher the DMSO2 content was, the larger the specific capacitance was, and the C_s value of 42.7 F/g was obtained on PCNF(2:3) electrode.

The specific capacitances of the PCNF electrodes were measured in 0.5 g/L NaCl in order to compare the effect of the salt concentration on the capacitor behavior. The CV curves in 0.5 g/L NaCl solution (Fig. S5A, SI) presented a obvious deformation and the corresponding capacitances were much lower than that at high NaCl concentration (Table 2). The faradic-like current probably from some active groups on the carbon surface is non-ignorable due to low double layer capacitance current (Fig. S5B, SI). The capacitance behavior on different PCNF electrodes can not be easily differentiated. Therefore, the high concentration solution is more suitable for double layer behavior characterization.

Fig. 5B showed the normalized CV curves of PCNF (2:3) electrode at different scan rates in 58.5 g/L NaCl solution. With the increase of the scan rate, the electrode maintains the characteristic of the double layer capacitor, but the specific capacitance reduced gradually. It indicates the restriction of the ionic transportation. On the PCNF (3:2) and PCNF (1:1) electrodes, this restriction becomes more serious (Fig. S6). Fig .6 showed the specific capacitance of different PCNF electrodes as a function of scan rates. The capacitance of PCNF (3:2) electrode is the highest at a low scan rate of 1 mV/s, while decreases dramatically with increasing the scan rate owing to the domination of

micropores as confirmed by pores distribution in Table 1. PCNF (2:3) had a slow decrease attributed to the mesoporous structure which facilitated the ions diffusion.

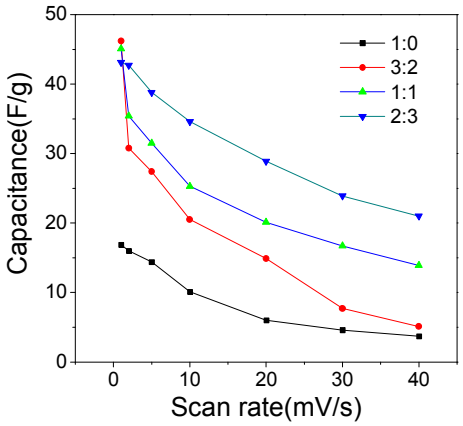

Fig 6. Specific capacitance of different PCNF electrodes as a function of scan rates

3.3 Capacitive deionization measurements

As discussed above, DMSO2 addition resulted in the formation of the porous carbon nanofibers. The desalination application of the resultant PCNFs was evaluated via assembling capacitors using PCNFs as free-standing electrodes. The cell was first cycled in 0.5 g/L NaCl aqueous solution overnight to reach the physical adsorption balance before desalination. During the charging－discharging process, the conductivity of the solution in the CDI cell was monitored by a conductivity meter. All the tests were performed at constant-current mode with the terminal voltage of 1.2 V. Fig.7 shows the continuous conductivity variation of solution during the charging-discharging process of different capacitors. The conductivity decreased during the charging process of the capacitor system, and the regeneration of the electrodes was achieved accompanying with desorption of salt during the discharging process. By comparison, the conductivity variations of solution in the CDI cell containing PAN/DMSO2 based PCNF (3:2, 1:1, 2:3)

electrodes were much higher than that for the PAN based PCNF(1:0) electrode. And the high DMSO2 dosage resulted in the enhanced conductivity variation. Based on the relationship of the conductivity and NaCl concentration described previously, the desalination amount per cycle and the coulomb efficiency for different electrodes were calculated and presented in Table 2. Clearly, the desalination amount of the PCNF electrode increased with the increase of DMSO2 ratio. The desalination amount of 8.1 mg/g was obtained for the PCNF (2:3) electrode. Interestingly, the coulomb efficiency has also some increase, probably due to the facile ionic diffusion through the mesopores. The comparative results about the desalination performance with previously reported self-supporting PCNF electrodes were summarized in Table 3. The proposed PCNF electrode is much better than the carbon black or graphene composited CNF, and comparable to the physically activated CNF. The effective capacitive deionization performance on the PCNF electrodes indicates that the mesoporous structure produced by DMSO2 evaporation contributes a lot to the enhancement of the salt adsorption performance. These results are in good agreement with the BET specific area and CV tests. Moreover, the proposed PCNF electrode is easy to fabricate without any activation process; the pore-forming agent DMSO2 can be easily recovered and reused, as confirmed in SI (Fig. S1 and Fig. S2). It concludes that the electrospun PAN/DMSO2 based PCNF can be used as a good electrode material for desalination application.

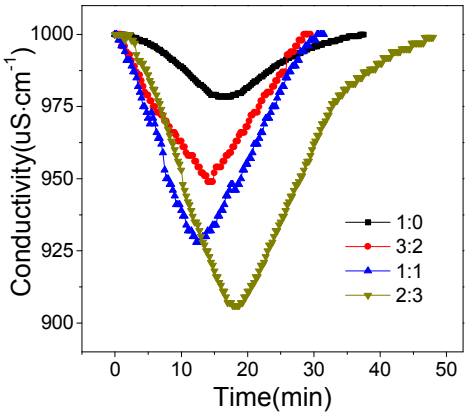

Fig.7. the conductivity variation of the solution with time during charge-discharge process of the capacitors containing different PCNF (1:0, 3:2, 1:1, 2:3) electrodes in 0.5 g/L NaCl solution.

Table 2 Capacitor characteristics of different PCNF electrodes

Electrodes	C^{a} (F/g)	C^{b} (F/g)	Desalination[c] (mg/g)	Coulomb efficiency (%)
PCNF(1:0)	16.1	6.1	1.7	30
PCNF(3:2)	30.8	10.1	4.1	40.4
PCNF(1:1)	35.4	12.1	6.2	44.2
PCNF(2:3)	42.7	13.8	8.1	57.8

[a] From CV in 58.5 g/L NaCl solution at 2 mV/s; [b] from CV in 0.5 g/L NaCl solution at 2 mV/s;
[c] Average desalination per cycle

Table 3 Comparison of the desalination performance on different carbon nanofiber electrodes

Original Material	Initial NaCl conc. (mg/L)	Operation voltage (V)	Salt adsorption (mg/g)	Activation	Ref.
ACNF	81	1.6	4.6	CO_2	23
ACNF	500	1.2	10.5	$ZnCl_2$	28
GO/ACNF	450	1.2	13.2	steam	49
CNT/ ACNF	400	1.2	6.4	CO_2	50
PhR-based CNF	2000	1.2	50	-	51
CB/ ACNF	90	1.6	9.13	CO_2	52
PMMA/CNF	45	1.2	1.9	-	53
rGO/ACNF	400	1.2	7.2	CO_2	54
DMSO2/PCNF	500	1.2	8.1	-	This work

The regeneration and stability of the electrode were investigated by recycling the CDI

cell with a charging and discharging alternate mode in 0.5 g/L NaCl solution. The continuous charging-discharging process was monitored by simultaneously recording voltage and conductivity, as shown in Fig 8. In short-circuit discharging process, the cell voltage decreased with the ions desorbing from the electrode, and electrode regeneration wasachieved with the final discharge voltage close to zero. Repeated charging-discharging test indicates that the PAN/DMSO2 based PCNF electrodes are very stable and can be regenerated completely.

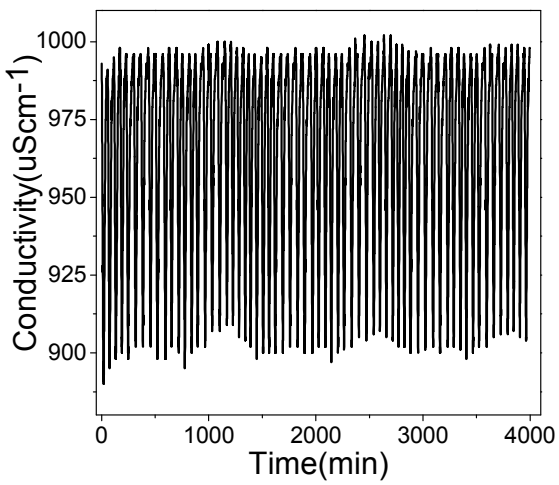

Fig.8. Conductivity variation with time in the PCNF (2:3)-based capacitor during the continuous charge-discharge process

4. Conclusion

In summary, using DMSO2 as additive, the porous carbon nanofiber has been fabricated successfully. The formation of pores on the nanofibers originates from evaporation removal of DMSO2 at the preoxidation stage. The pore distribution depends on the DMSO2 content. Compared with the pure PAN-based CNF electrodes, the electrochemical properties and the desalination amount of the PCNF electrodes were

greatly improved because of the suitable micro/meso structure contribution. This work provides an efficient, economical and simple approach to fabricate the porous carbon nanofiber electrodes without additional treatment. More detailed studies such as the effect of polymer types on pore structure in other DMSO2-containing nanofiber system are still under way.

Acknowledgements:

This work was financially supported by the National Science Foundation (No.21105009, No.21476047) and the State Key Laboratory of the Electroanalytical Chemistry Foundation (SKLEAC202105).

References :

1. US Pat.,5547581-A,1996.
2. US Pat.,6778378-B1,2004.
3. Y. Oren, *Desalination*, 2008, 228, 10-29.
4. S. Porada, R. Zhao, A. van der Wal, V. Presser and P. M. Biesheuvel, *Prog. Mater. Sci.*,2013, 58, 1388-1442.
5. L. F. Greenlee, D. F. Lawler, B. D. Freeman, B. Marrot and P. Moulin, *Water Res.*,2009, 43, 2317-2348.
6. K. P. Lee, T. C. Arnot and D. Mattia, *J. Membr. Sci.*, 2011, 370, 1-22.
7. L. J. Banasiak, T. W. Kruttschnitt and A. I. Schäfer, *Desalination*, 2007, 205, 38-46.
8. I. Cohen, E. Avraham, A. Soffer and D. Aurbach, ESC Trans., 2012, 45, 43-59.
9. US Pat.,5779891-A,1998.

10. M. Mossad and L. Zou, *J. Hazard. Mater.*, 2012, 213-214, 491-497.

11. A. G. Pandolfo and A. F. Hollenkamp, *J. Power Sources*, 2006, 157, 11-27.

12. M. Andelman, *J. Mater. Sci. Chem. Eng.*, 2014, 02, 16-22.

13. L. Zou, G. Morris and D. Qi, *Desalination*, 2008, 225, 329-340.

14. J.-H. Choi, *Sep. Purif. Technol.,* 2010, 70, 362-366.

15. P. Xu, J. E. Drewes, D. Heil and G. Wang, *Water Res.*, 2008, 42, 2605-2617.

16. H.-H. Jung, S.-W. Hwang, S.-H. Hyun, K.-H. Lee and G.-T. Kim, *Desalination*, 2007, 216, 377-385.

17. C. J. Gabelich, T. D. Tran and I. H. Suffet, *Environ. Sci. Technol.*, 2002, 36, 3010-3019.

18. C. Nie, L. Pan, H. Li, T. Chen, T. Lu and Z. Sun, *J. Electroanal. Chem.*, 2012, 666, 85-88.

19. D. Zhang, L. Shi, J. Fang and K. Dai, *J. Mater. Sci.*, 2006, 42, 2471-2475.

20. D. Zhang, T. Yan, L. Shi, Z. Peng, X. Wen and J. Zhang, *J. Mater. Chem.*, 2012, 22, 14696.

21. H. Wang, L. Shi, T. Yan, J. Zhang, Q. Zhong and D. Zhang, *J. Mater. Chem. A*, 2014, 2, 4739.

22. C. Yan, Y. W. Kanaththage, R. Short, C. T. Gibson and L. Zou, *Desalination*, 2014, 344, 274-279.

23. G. Wang, C. Pan, L. Wang, Q. Dong, C. Yu, Z. Zhao and J. Qiu, *Electrochim. Acta*, 2012, 69, 65-70.

24. A. G. El-Deen, N. A. M. Barakat, K. A. Khalil and H. Y. Kim, *J. Mater. Chem. A*,

2013, 1, 11001.

25. D. Li and Y. N. Xia, *Adv. Mater.*, 2004, 16, 1151-1170.

26. S. K. Nataraj, K. S. Yang and T. M. Aminabhavi, *Prog. Polym. Sci.*, 2012, 37, 487-513.

27. M. S. A. Rahaman, A. F. Ismail and A. Mustafa, *Polym. Degrad. Stab.*, 2007, 92, 1421-1432.

28. J. Liu, S. Wang, J. Yang, J. Liao, M. Lu, H. Pan and L. An, *Desalination*, 2014, 344, 446-453.

29. M. Wang, Z.-H. Huang, L. Wang, M.-X. Wang, F. Kang and H. Hou, *New J. Chem.*, 2010, 34, 1843-1845.

30. C. Kim, S. H. Park, W. J. Lee and K. S. Yang, *Electrochim. Acta*, 2004, 50, 877-881.

31. C. Kim and K. S. Yang, *Appl. Phys. Lett.*, 2003, 83, 1216-1218.

32. Q. H. Guo, X. P. Zhou, X. Y. Li, S. L. Chen, A. Seema, A. Greiner and H. Q. Hou, *J. Mater. Chem.*, 2009, 19, 2810-2816.

33. E. J. Ra, E. Raymundo-Pinero, Y. H. Lee and F. Beguin, *Carbon*, 2009, 47, 2984-2992.

34. B. Xu, F. Wu, R. J. Chen, G. P. Cao, S. Chen and Y. S. Yang, *J. Power Sources*, 2010, 195, 2118-2124.

35. E. Jo, J.-G. Yeo, D. K. Kim, J. S. Oh and C. K. Hong, *Polymer International*, 2014, 63, 1471-1477.

36. H. Niu, J. Zhang, Z. Xie, X. Wang and T. Lin, *Carbon*, 2011, 49, 2380-2388.

37. C. Tran and V. Kalra, *J. Power Sources*, 2013, 235, 289-296.

38. S. Porada, L. Borchardt, M. Oschatz, M. Bryjak, J. S. Atchison, K. J. Keesman, S. Kaskel, P. M. Biesheuvel and V. Presser, *Energy Environ. Sci.*, 2013, 6, 3700.

39. W. Qing-Yun, W. Ling-Shu and X. Zhi-Kang, *Polymer*, 2013, 54, 284-291.

40. Q.-Y. Wu, L.-S. Wan and Z.-K. Xu, *J. Membr. Sci.*, 2012, 409-410, 355-364.

41. L. Hong-Qing, W. Qing-Yun, W. Ling-Shu, H. Xiao-Jun and X. Zhi-Kang, *J. Membr. Sci.*, 2013, 446, 482-491.

42. Z. F. J. Yan, T. Wei, J. Cheng, B. Shao, K. Wang, L. Song, M. Zhang, *J. Power Sources,* 2009, 194, 1202.43. V. Presser, J. McDonough, S.-H. Yeon and Y. Gogotsi, *Energy Environ. Sci.*, 2011, 4, 3059.

44. X. Xie and L. Gao, *Carbon*, 2007, 45, 2365-2373.

45. G. Wang, C. Pan, L. Wang, Q. Dong, C. Yu, Z. Zhao and J. Qiu, *Electrochim. Acta*, 2012, 69, 65-70.

46. L. Ji and X. Zhang, *Mater. Lett.*, 2008, 62, 2161-2164

47. Q.-Y. Wu, L.-S. Wan and Z.-K. Xu, *RSC Adv.*, 2013, 3, 17105.

48. G. Hasegawa, M. Aoki, K. Kanamori, K. Nakanishi, T. Hanada and K. Tadanaga, *J. Mater. Chem.*, 2011, 21, 2060.

49. Y. Bai, Z.-H. Huang, X.-L. Yu and F. Kang, *Colloids Surf., A*, 2014, 444, 153-158.

50. Q. Dong, G. Wang, T. Wu, S. Peng and J. Qiu, *J. Colloid Interface Sci.*, 2015, 446, 387-392.

51. Y. Chen, M. Yue, Z.-H. Huang and F. Kang, *Chem. Eng. J.*, 2014, 252, 30-37.

52. G. Wang, Q. Dong, Z. Ling, C. Pan, C. Yu and J. Qiu, *J. Mater. Chem.*, 2012, 22,

21819.

53. A. G. El-Deen, N. A. M. Barakat, K. A. Khalil and H. Y. Kim, *New J. Chem.*, 2014, 38, 198-205.

54. Q. Dong, G. Wang, B. Qian, C. Hu, Y. Wang and J. Qiu, *Electrochim. Acta*, 2014, 137, 388-394.

Table of contents:

Flexible porous CNF *via* facile heat treatment of electrospun PAN/DMSO2 nanofibers was successfully used for CDI with excellent desalination performance.